ORIGINAL RESEARCH

In Vivo Detection of Cortical Plaques by MR Imaging in Patients with Multiple Sclerosis

F. Bagnato
J.A. Butman
S. Gupta
M. Calabrese
L. Pezawas
J.M. Ohayon
F. Tovar-Moll
M. Riva
M.M. Cao
S.L. Talagala
H.F. McFarland

BACKGROUND AND PURPOSE: In vivo detection of cortical lesions in patients with multiple sclerosis (MS) by MR imaging is hampered by several factors. Among them is the low contrast between small cortical lesions and surrounding cortical gray matter offered by present techniques.

METHODS: T1-weighted 3D spoiled gradient-recalled-echo (SPGR) volumes and 2D fluid-attenuated inversion recovery (FLAIR) sequences of 22 patients with MS who had 12 monthly brain MR imaging examinations at 1.5T, using a quadrature head coil, were retrospectively analyzed. These serial studies were coregistered and averaged to generate a single high signal-to-noise ratio (SNR) mean image, which was used to identify cortical lesions. The means of 12 FLAIRs and SPGRs from 14 age- and sex-matched healthy volunteers were analyzed as well.

RESULTS: No cortical lesions were found on images of healthy subjects. Eighty-six cortical lesions were identified in 13 (59.1%) patients, predominantly in the frontal lobe (73.3%); 23.3% of cortical lesions lay entirely in the cortex, whereas the remaining lesions invaded the white matter underneath.

CONCLUSION: Averaging multiple SPGRs created a single high SNR volume, allowing identification of cortical lesions. Because data were obtained monthly for 1 year, the average image does not account for transient lesion activity. However, for cortical lesions that remained stable during this time, the findings are valid in demonstrating the importance of high SNR images for detecting cortical brain abnormalities in MS.

Active and chronic cortical lesions either entirely lying in the cortex or touching the abutting white matter are described in postmortem studies on patients with multiple sclerosis (MS).[1-6] However, in vivo detection of cortical lesions is still challenging. Cortical lesions are small and exhibit a low contrast with respect to the surrounding gray matter. Thus high signal-to-noise ratio (SNR) images with corresponding high contrast-to-noise ratio (CNR) between tissues or between normal and abnormal areas are crucial to identify cortical lesions.

In earlier studies, it was shown that 2D-fluid-attenuated inversion recovery (FLAIR) images may slightly improve juxtacortical lesion detection.[7-11] By zeroing the signal intensity derived from the CSF, 2D-FLAIR images revealed lesions more accurately in the proximity of the cortex in patients with MS. Recently, a relative gain of 152% in the detection of cortical lesions was achieved by using a double inversion-recovery sequence suppressing the CSF and white matter signals at the same time, compared to a 3D-FLAIR sequence.[12] Both FLAIR and double inversion recovery image techniques used in previous studies are weighted towards the T2 parameters. However, T1-weighted images have the potential to clearly visualize gray matter/white matter boundaries which are not as clearly distinguishable on T2-weighted images. Therefore, the current study evaluated cortical lesions on high-resolution T1-weighted 3D-spoiled gradient-recalled-echo (SPGR) and FLAIR images at the same time.

The main purpose of the present work was to test the hypothesis that T1-weighted images with high SNR would allow identification of cortical lesions not otherwise visible in patients with MS. To test this hypothesis, we retrospectively examined pre-existing images from patients already enrolled in clinical trials or natural history studies at the neuroimmunology branch (NIB), where high-resolution T1-SPGR sequences are obtained as part of the MS standard MR imaging protocol.

We hypothesized that 1) coregistration of multiple 3D volume SPGRs and FLAIRs would be similar to performing MR imaging with multiple excitations and that the commensurate improvements in SNR would allow for the clear depiction of small cortical lesions in MS despite the inherently lower lesion contrast; and that 2) demarcation of the gray-white boundary on T1-SPGR will permit categorization of MS plaques as intracortical or transcortical.

Methods

Patients and Study Design

The present work was performed at the National Institutes of Health (NIH) in Bethesda, Md, with the approval of the Institutional Review Board of the National Institute of Neurologic Disorders and Stroke (NINDS). Each patient and healthy volunteer signed an informed consent. This was a retrospective study evaluating multiple SPGRs and FLAIRs of 22 patients with MS. Both sequences were part of the standard MR imaging MS protocol performed in the NIB MS clinic on a regular basis. No selection criteria were used for the purpose of the present study, and all patients with MS, referred to the NIB of NIH

Received December 12. 2005; accepted after revision February 3, 2006.

From the Neuroimmunology Branch (F.B.*, S.G., M.C., J.M.O., F.T.-M., M.R., M.M.C., H.F.M.), NINDS, and the Diagnostic Radiology Department (J.A.B.*), Warren G. Magnuson Clinical Center, NIH, Bethesda, Md; New York Medical College (S.G.), Valhalla, NY; Genes, Cognition and Psychosis Program (L.P.), NIH, Bethesda, Md; and NIH-MRI Research Facility (S.L.T.), NINDS, NIH, Bethesda, Md.

*These 2 Authors contributed equally to the work.

This work was supported by the Intramural Research Program of the NINDS-NIH. The contribution of author M.M. Cao was facilitated by a fellowship with the Clinical Research Training Program, a public-private partnership supported jointly by the NIH and a grant to the Foundation for the NIH from Pfizer Pharmaceuticals Group. M. Calabrese received a public research grant from the University of Padova in Italy.

Presented as oral communication at: Annual Meeting of the American Society of Neuroradiology, June 2004; Seattle, Wash., and in poster format at: Annual Meeting of the American Academy of Neurology, April–May 2004; San Francisco, Calif.

Address correspondence to Francesca Bagnato, MD, NIB-NINDS-NIH, 10 Center Dr, Bldg 10, Room 5B16, Bethesda, MD 20892-1400; e-mail: bagnatof@ninds.nih.gov

Table 1: Demographic, clinical, and MRI characteristics of patients

	Patients (n = 22)	Healthy Volunteers (n = 12)
Age*†	40.3 ± 8.8 (22−57) years	41.5 ± 11.2 (28−58) years
Gender†	16 women; 6 men	6 women; 6 men
MS type	10 SPMS;12 RRMS	
Disease duration*	9.8 ± 8.2 (0.2−26.1) years	
EDSS score*	3.3 ± 1.9 (0−7.0) [baseline]	
	3.4 ± 2.1 (0−6.5) [end]	
Number of CELs*	41.2 ± 82.9 (0−345) [total]	
T2 lesions volume* (cm^3)	16.2 ± 16.9 (1.2−68.2) [baseline]	
	14.38 ± 15.2 (0.7−52.0) [end]	
T1 BHs number*	10.3 ± 8.9 (0−37) [baseline]	
	10.5 ± 10.1 (0−39) [end]	
T1 BHs volume* (cm^3)	1.8 ± 2.0 (0−7.5) [baseline]	
	1.9 ± 2.3 (0−8.3) [end]	
BPF*‡	0.80 ± 0.02 (0.76−0.83) [baseline]	0.85 ± 0.01 (0.84−0.88)
	0.79 ± 0.02 (0.74−0.83) [end]	
On-going therapy	Cyclophoshamide = 1	
(4 untreated patients)	Copolimer-1 = 4	
	Interferon β (IFNβ) = 6	
	IFNβ + Daclizumab = 7	

Note:—MS indicates multiple sclerosis; RRMS, relapsing-remitting multiple sclerosis; SPMS, secondary-progressive multiple sclerosis; EDSS, expanded disability status scale; CEL, contrast-enhancing lesion; BH, black hole; BPF, brain parenchymal fraction.
* mean ± SD (range).
† P values vs healthy volunteers > .05.
‡ $P \leq .0001$. See text for comparisons within patients at different time points.

for either immunologic studies or consideration of enrollment in a therapeutic protocol with at least 12 monthly SPGRs were consecutively considered. Demographic, clinical, and MR imaging characteristics of patients at baseline are reported in Table 1. Each patient underwent monthly (±1 week) clinical examinations (disability rating with the Expanded Disability Status Scale ([EDSS] score)[13] and 1.5T brain MR imaging for 12 months.

Fourteen age- and sex-matched healthy volunteers were considered for this study as well. Each healthy volunteer underwent 12 MR imaging examinations that were obtained in 2 separate sessions over a 6-month period. Healthy volunteers' images were collected for comparisons of brain volumes with patients' brain size, as well as for assessing the absence of cortical signal intensity changes that could resemble abnormalities identified as lesions on patients' images.

MR Imaging Acquisition

Patients. Each patient underwent the standard MR imaging protocol used routinely at the MS clinic of NIB-NINDS-NIH. Precisely, for each MR imaging of the brain performed at 1.5T by using a quadrature head coil (GE Healthcare, Milwaukee, Wis), we obtained the following contiguous images: 1) T2-weighted spin-echo (SE) with variable TE, 20/100 ms; TR, 2000 ms; 2 excitations; matrix, 192 × 256; FOV, 24 cm; section thickness, 3 mm; 2) 2D FLAIR with TE,140 ms; TR, 10 000 ms; TI, 2200 ms; 1 excitation; matrix, 192 × 256; FOV, 24 cm; section thickness, 3 mm; 3) SE T1-weighted with a TE, 16 ms; TR, 600 ms; 2 excitations; matrix, 192 × 256; FOV, 24 cm; section thickness, 3 mm; 4) T1-weighted 3D-SPGR volumes; TE, minimum; TR, 9 ms; 1 excitation; flip angle, 20°; matrix, 256 × 256; FOV, 24 cm; bandwidth, 15.63 KHz; section thickness, 1.4 mm with a single 128-section acquisition; acquisition time, 4 minutes 42 seconds; and 5) postcontrast SE T1-weighted within 15 minutes after the injection of gadopentetate dimeglumine (Magnevist, Berlex Laboratories, Cedar Knolls, NJ) at 0.1 mmol/kg.

Healthy Volunteer Subjects. Twelve T1-weighted 3D-SPGR volumes and FLAIR images were obtained with a 1.5T magnet in healthy volunteers by using the same parameters as those used for patients. MR imaging acquisitions for healthy volunteers were obtained in 2 separate sessions. During each session SPGR and FLAIR sequences were acquired 6 times (totaling 12 acquisitions). Within each session, the subject was removed from the scanner and repositioned after each acquisition, to mimic the misalignment of images in patients whose data were obtained in 12 separate monthly sessions. Time length covering the MR imaging performed in patients and healthy volunteers was different. However, because the main goal of imaging healthy volunteers was achieving an adequate volume/image with an SNR comparable to the one gained by averaging 12 monthly SPGRs in patients and verifying the hypothesis that no abnormalities could be detected in healthy individuals, we reasoned that for the purpose of the present study, such a difference might not affect the results and their interpretation.

Image Analysis

Data were stored in DICOM format, transformed to Analyze format and analyzed on a Linux workstation (Red Hat 8.0).

Postprocessing Analysis of 3D-SPGR Images and 2D-FLAIR Images. All available 12 SPGR images of each patient and healthy volunteer underwent nonuniformity intensity correction by using N3 software,[14] followed by Winsor filtering (spatial noise filtering)[15,16] by using Analysis of Functional Neuroimages (AFNI) (http://afni.nimh.nih.gov).[17] A conservative 1-voxel radius was chosen so as not to affect lesions significantly. This was followed by a weighted least squares cost-function coregistration of all images to the baseline image for each subject using the routine '3dvolreg' in AFNI.[18] A mean image of each subject was created by using statistical tools available in AFNI. Lesion localization was double-checked on mean images obtained before and after the averaging and warping into Talairach space.[19]

An automated image-registration algorithm that enabled registration of successive FLAIR MR images to the mean 3D SPGR was used for each patient and healthy volunteer by applying a linear image-registration tool as developed at the Oxford Centre for Functional Magnetic Resonance Imaging of the Brain (FMRIB) (http://www.

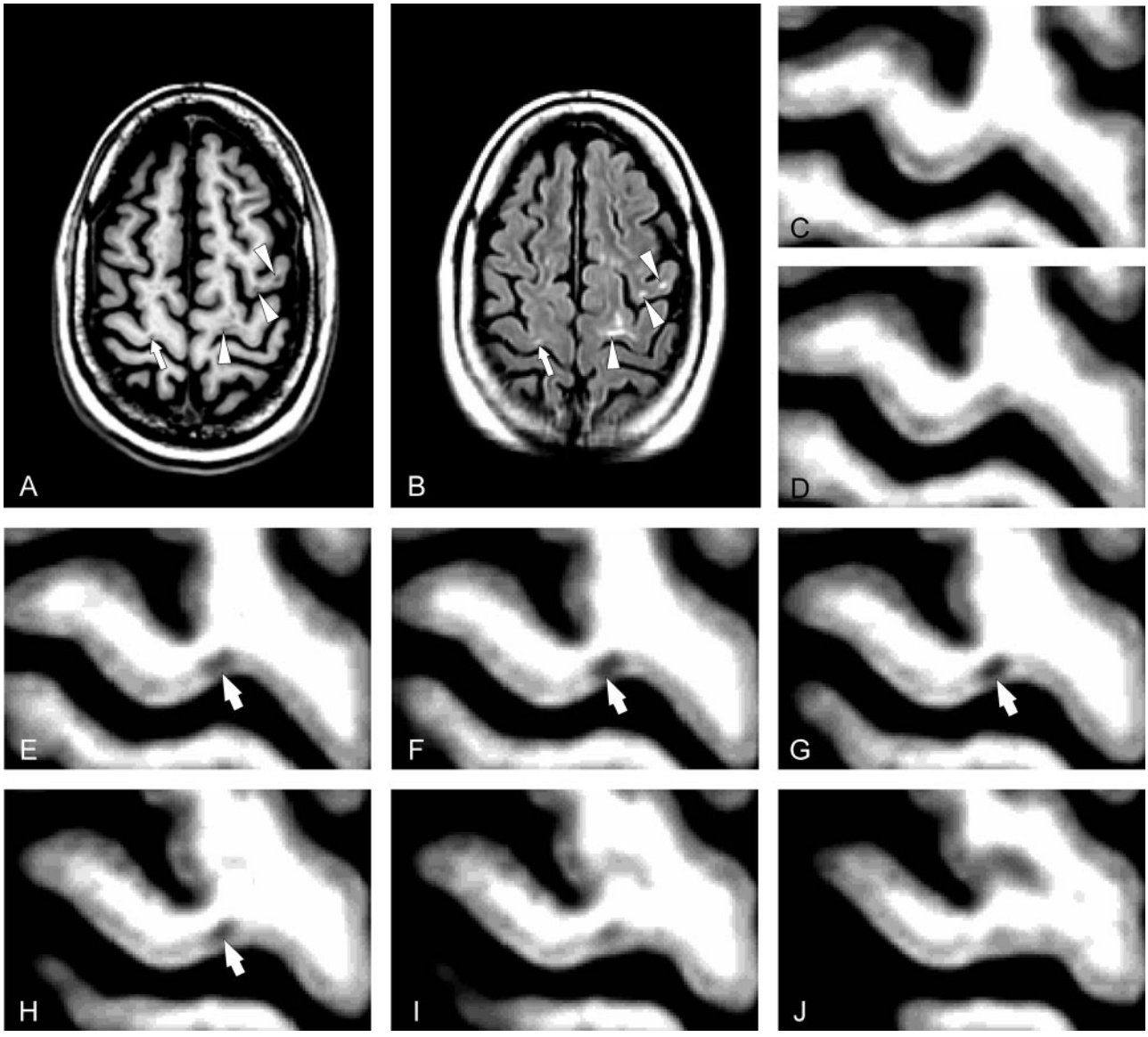

Fig 1. Average of 12 coregistered axial SPGR (*A*) and FLAIR (*B*) MR images demonstrate cortical MS lesions in patient 3. Several Type B cortical lesions traverse the gray-white boundary (*white arrowheads, A, B*). A single Type A lesion (*white arrows A, B*) is confined to the gray matter of the motor strip. Serial magnified images of the precentral gyrus (*C-J*) conform that this lesion (*white arrows D-H*) does not extend into the juxtacortical white matter.

fmrib.ox.ac.uk/).[20] Subsequently, the creation of a mean 2D-FLAIR image for each patient and healthy volunteer was carried out by using statistic tools available in MEDx 3.4.3 (http://mfs0.cc.nih.gov).

Accuracy of image registration was visually inspected by 2 investigators who carefully analyzed all mean and SD images of each individual.

CNR Evaluations of 3D-SPGR Images. CNR of a single SPGR and mean of 12 averaged SPGR volumes were evaluated on data from 6 healthy volunteers. For each image, 12 regions of interest (ROIs) were placed bilaterally in 4 regions of white matter (65.9 mm^2), 4 regions of cortical gray matter (14.1 mm^2), and 4 regions outside the brain and away from imaging artifacts (140.6 mm^2). CNR was given by the following formula: $(S_{wm} - S_{gm})/\sigma$, where S_{wm} and S_{gm} are the mean signal intensities of each white matter and gray matter ROI, respectively, and σ is the mean of the SDs signal intensity in each ROI outside the brain.

Identification of Cortical Lesions. Cortical lesions were identified on the average SPGR image created by 12 coregistered 3D volume MR images and confirmed on the mean FLAIR image created by 12 coregistered FLAIR MR images by 2 physicians who reached an interobserver variability equal to 0.1%. Both physicians were blinded with respect to clinical characteristics of individual patients but were obviously aware of the white matter lesions of patients. Cortical lesions were abnormalities visible as hypointense on the mean 3D-SPGR image and confirmed as hyperintense on the mean 2D-FLAIR image. Two types of cortical lesions were identified: Type A cortical lesions were defined as those lesions entirely confined to the cortical tissue (Fig 1). Type B cortical lesions were those lesions lying predominately within the cortex, with some extension into the white matter (Figs 1 and 2).

Lesions and Brain Volume Computation. T1 and T2 lesions, as well as brain volume, were analyzed on first and last MR images. Computation of T1-hypointense lesions, or black holes,[21] was performed by using a semiautomated procedure available in MEDx 3.4.3 by 1 physician.[22] T2-hyperintense lesions were identified and computed by the means of a segmentation tool available in Medical Image Processing, Analysis, and Visualization (MIPAV) developed at NIH

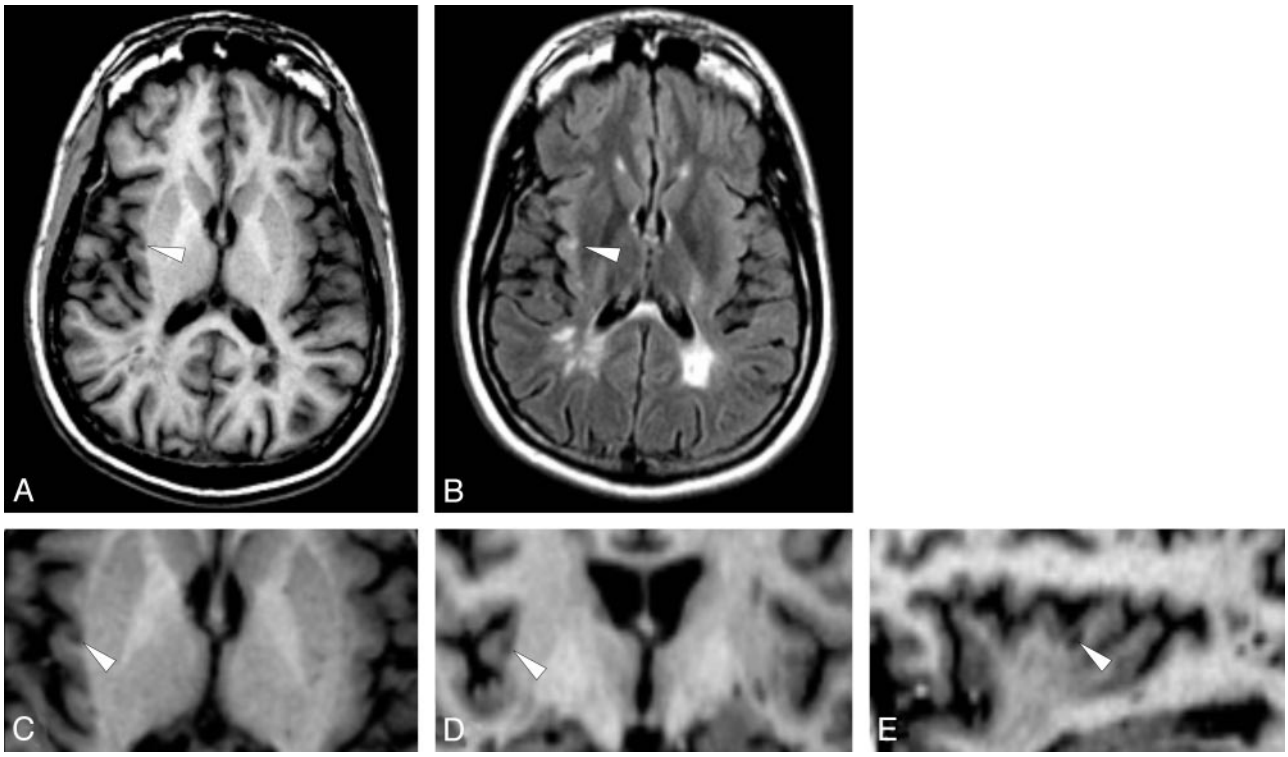

Fig 2. Average of 12 coregistered SPGR (*A*) and FLAIR (*B*) demonstrate a Type B cortical lesion in the right insula (*arrowheads*). Higher magnification of the averaged SPGR dataset in the axial (*C*), coronal (*D*), and sagittal (*E*) planes shows the relationship of the lesion to the cortical ribbon. (Patient 2).

(http://mipav.cit.nih.gov/)[23] by 1 investigator. Brain parenchymal fraction (BPF) was computed for the initial and last brain 3D-SPGR images of each patient and healthy volunteer by using MIPAV. The brain extraction tool as developed by FMRIB was first used to extract the brain.[24] Manual editing was required to delete regions of nonbrain tissue that the software was unable to identify and was performed by a physician. Fuzzy-connectedness segmentation was then used to segment gray matter, white matter, CSF, and background.[23] BPF was calculated by using the formula: BPF = (gray matter + white matter) / (white matter + gray matter + CSF).[25,26]

Total number and new contrast-enhancing lesions (CELs) were identified and sequentially numbered on the 12 monthly hard copy films by 2 experienced readers.

Statistical Analysis

The coefficient of variation of the various MR imaging measurements was calculated by dividing the corresponding SD by the mean. Fisher exact tests were performed to determine differences in the sex distribution between patients and healthy volunteers as well as differences in sex distribution and MS type between patients with MS with and without cortical lesions. Mann-Whitney *U* tests were performed to determine differences in age and BPF between patients with MS and healthy volunteers. Mann-Whitney *U* tests were also used to determine differences in ages, disease duration, EDSS scores, numbers and volumes of T1 hypointensities, T2 FLAIR hyperintensities, BPFs, and total CELs between MS patients with and without cortical lesions. All reported *P* values were based on 2-tailed statistical tests, with a significance level of 0.01 to account for the multiple comparisons. Bonferroni correction was not used because of the exploratory nature of the study, and the multiple comparisons did not fall within a single joint family of comparisons by definition.

As shown in the "Results" section, given the small number of cortical lesions identified in individual patients and the exploratory nature of the present study, we could not perform correlation analysis between the number of cortical lesions and other MR imaging metrics. The statistical analyses were performed by using SPSS Version 12.0 (SPSS, Chicago, Ill).

Results

CNR Measurements

An increase in CNR greater than threefold was observed when comparing a single section to the 12-averaged dataset. Mean ± SD (range) CNR of 1 and 12-averaged SPGRs were as follows: 8.7 ± 2.5 (6.2–11.5) and 23.9 ± 5.0 (17.5–29.5). The increasing conspicuity of lesion identification is clearly identifiable in Fig 3.

Incidence and Distribution of Cortical Lesions

None of the healthy volunteers presented with cortical lesions.

Cortical lesions were found in 13 (59.1%) patients whose individual demographic, clinical, and MR imaging characteristics are listed in Table 2. Nine (40.3%) of these patients were found with at least 1 type A cortical lesion. A total of 86 cortical lesions was identified; 20 (23.3%) of the cortical lesions were lying entirely in the cortex without invading the white matter. The remaining 66 (76.7%) cortical lesions traversed the white matter to some extent. The distribution of the types of cortical lesions is presented in Table 3. Most identified cortical lesions were located in frontal lobe areas (63/86 cortical lesions, 73.3%). Fifteen lesions were identified in deeper gray matter structures outside the cortex. Distributions of those lesions were as follows: 4 in the lentiform nuclei, 3 in the thalamus, 3 in the caudate, 2 in the putamen, 1 in the amygdala, 1 in the tuber cinereum, and 1 in the cerebellar cortex.

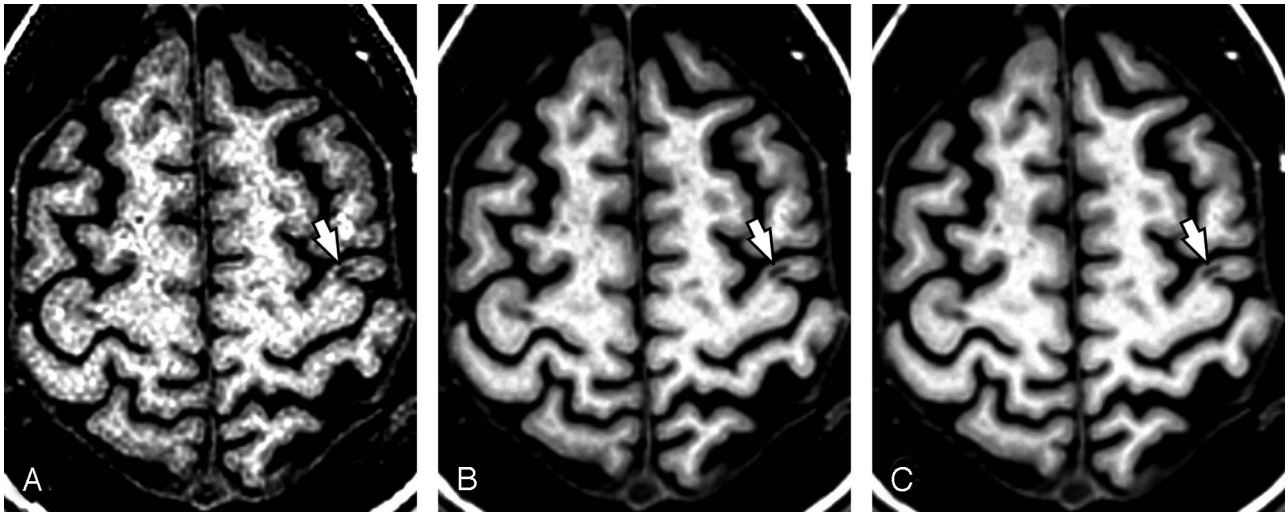

Fig 3. Coregistration and averaging 6 (*B*) and 12 (*C*) T1 SPGR MRI volumes improves conspicuity of cortical lesions (e.g. Type B lesion *arrows, A-C*) relative to a single SPGR (*A*). Although the Type B lesion is visible on the single SPGR (*A*), coregistering and averaging 6 (*B*) and 12 (*C*) SPGRs improves lesion conspicuity, and allows clear characterization of lesion location with respect to the gray-white boundary. (Patient 6).

Table 2: Demographic, clinical, and MRI characteristics of patients with cortical lesions at the study entry

Pt #	Age	Gender	Years of MS	EDSS	MS type	T1 Les Volume (cm^3)	T2 Les Volume (cm^3)	CELs	BPF	CLs(A)	CLs(B)
1	35.2	Male	9	5.5	SP	4.4	12.5	0	0.77	0	2
2	35.7	Male	3.4	0	RR	0.8	19.2	6	0.78	1	6
3	35.8	Male	4.7	1.5	RR	1.4	12.1	0	0.78	3	7
4	36.9	Female	15.4	2.5	RR	1.6	16.9	NA	0.81	1	7
5	50.3	Female	8.9	6	SP	2.4	15.2	4	0.82	0	10
6	48.6	Female	24	2.5	RR	4.1	42.2	2	0.77	2	3
7	42.7	Female	0.3	1.5	RR	0.1	2.6	1	0.82	0	3
8	41.2	Female	25.2	4.5	SP	1.2	18.6	1	0.77	1	5
9	48.3	Female	6.1	2.5	SP*	2.5	68.3	26	0.76	5	1
10	26.5	Female	13	6	SP	7.5	25.6	0	0.76	2	0
11	56.6	Female	18.9	6.5	SP	1.4	6.3	2	0.68	1	7
12	22.3	Male	2	3	RR	4.2	44.70	3	0.81	4	13
13	35.7	Female	11.9	5	SP	0.2	1.2	0	0.82	0	2

Note:—MS indicates multiple sclerosis; RR, relapsing-remitting; SP, secondary-progressive; EDSS, expanded disability status scale; CEL, contrast-enhancing lesion; CL, cortical lesion; BPF, brain parenchymal fraction; NA, not available; Les, lesion.
* Relapsing-progressive MS.

Table 3: Site and type of cortical lesions

	Number (% of total) Cortical Lesions	Type A	Type B
Superior frontal gyrus	17 (19.8%)	2	15
Middle frontal gyrus	25 (29.1%)	6	19
Inferior frontal gyrus	3 (3.5%)	1	2
Precentral gyrus	18 (20.5%)	6	12
Postcentral gyrus	3 (3.5%)	0	3
Precuneus	2 (2.3%)	1	1
Superior parietal lobe	2 (2.3%)	0	2
Supramarginal gyrus	1 (1.2%)	0	1
Inferior parietal lobe	2 (2.3%)	0	2
Insula	2 (2.3%)	0	2
Superior temporal gyrus	5 (6.8%)	2	3
Inferior temporal gyrus	1 (1.2%)	0	1
Parahippocampal gyrus	2 (2.3%)	0	2
Uncus	2 (2.3%)	1	1
Cuneus	1 (1.2%)	1	0
Total	86	20	66

Clinical and MR Imaging Differences Between Patients With and Without Cortical Lesions

Age, sex distribution, disease duration, baseline, and end EDSS score and MS type frequency did not significantly differ between patients with and without cortical lesions. On examining MR imaging variables, we found that only the T2 lesion loads at the first ($P = .001$) and last ($P = .002$) MR imaging were greater among patients with MS with cortical lesions in comparison with patients without cortical lesions at both the baseline and the study end scan. However, such a difference was observed only when patients with at least 1 type A cortical lesion (ie, 9/22) were compared with patients with only type B cortical lesions and those without cortical abnormalities considered as a group. No MR imaging and clinical differences between patients with both type A and B cortical lesions and patients without cortical lesions were observed.

Discussion

Identification of cortical lesions has special importance for patients with MS. First, cortical lesions may have the potential

to explain more accurately the basis of clinical disability in patients. Second, quantification of cortical lesions could be an additional extremely relevant tool for monitoring experimental treatments with potential neuroprotective effects.

Averaging multiple SPGRs created a single high SNR volume, allowing identification of cortical lesions. Because those sequences were not initially designed to achieve a high SNR (ie, 1 NEX and approximately 5 minutes of acquisition time), we averaged 12 consecutive MR images to demonstrate lesion conspicuity.

Because data were obtained monthly for 1 year, it is expected that some lesions changed with time and the average image may not appropriately depict these lesions. However, because of the marked improvement in lesion SNR, intracortical lesions as well as mixed cortical lesions that remained stable during this time were unambiguously identified in our cohort of patients with MS.

A total of 86 cortical lesions in approximately 60% of the patients was identified. As shown in a recent pathologic report,[27] an association between white matter lesion load and the presence of cortical lesions was found. Particularly, greater T2 lesion volumes in patients with cortical lesions were observed when the MS cohort was restricted to patients with purely intracortical lesions. As one can see in Table 2, 50% of the patients with cortical lesions were in the secondary-progressive (SP) course of disease, thus differences in distributions of patients with SPMS and relapsing-remitting MS were not significant. An association between the presence of cortical lesions and higher disability scores could also not be demonstrated. One can postulate that our small sample size did not provide enough statistical power to detect the clinical impact of focal cortical pathology. On the contrary, however, focal cortical pathology was still found in some of our patients with early MS (ie, approximately 4 months from disease onset) and very low or absent disability. This suggests that as seen for diffuse cortical disease, focal cortical pathology may start early in some patients, and it confirms previous results of early diffuse involvement of cortical pathology.[28,29]

Cortical lesions were distributed in almost all cortical areas of the brain with a higher prevalence found in frontal lobe associative areas as well as primary/secondary motor regions. The high distribution of cortical lesions in the superior/medial gyrus may be an additional factor responsible for the lack of correlation between the presence of cortical lesions and higher EDSS score. Indeed, those areas are responsible for cognitive functions, which are not adequately and precisely assessed by the EDSS score.

As for the involvement of cortical lesions in the frontal motor area, our data are in concordance with previous studies that found the greatest regional cortical thickness variations in similar frontal lobe regions of patients with MS. One could speculate a higher disease susceptibly for these regions.[30,31] However, the fact that motor areas are potentially better visualized because of their greater thickness compared with other regions of the cerebral cortex[32] needs to be considered as potential bias in the interpretation of our and previous findings.

Most cortical lesions identified in our patients were present in both white matter and cortical gray matter (ie, type B cortical lesions), and only a minority of them existed exclusively within the cortex (ie, type A cortical lesions). The latter parallels results from some previous authors[2,7] but is not consistent with some previous neuropathologic studies in which higher proportions of intracortical lesions were found.[3-5] Care needs to be taken in the interpretation of our findings. Indeed, our results only describe cortical lesions that persisted across a timeframe of 1 year, which most likely represent only a small subset of the cortical lesions actually observed in cross-sectional postmortem evaluations. Hence, underestimation of intracortical lesions might have occurred. Indeed, in studies assessing the sensitivity of MR imaging in depicting cortical lesions against the standard of a neuropathologic examination, up to 44%, 22%, and 50% of intracortical lesions remained invisible on turbo SE, 3D FLAIR, and T1-weighted images, respectively.[6] Underestimation of Type A lesions may also be related to our conservative method for definitively identifying a cortical lesion, i.e. only lesions seen on both FLAIR and SPGR were counted. Given that the FLAIR images were twice as thick as the SPGR sequences, small intracortical lesions might not have been identifiable on the FLAIR sequence.

Although no definitive answer is provided by our findings on the role of cortical lesions in disability of patients with MS as well as on the true incidence of those abnormalities, we believe that our findings provide a basis for reporting that high SNR images are an excellent tool for in vivo lesion conspicuity.

Conclusions

Although not applicable in clinical practice or in prospective clinical trials, the methodology we used is still relevant, showing the advantage provided by high SNR images for detecting cortical lesions. Limitations of this method will be overcome in the future by acquiring MR imaging data at higher field strength (eg, 3T) and by using multichannel receive coils to improve the SNR of the 3D-SPGR and FLAIR images. In the future, aforementioned technical improvements will provide adequate image quality to detect cortical lesions in patients with MS by a single scan and to describe the dynamics of those abnormalities with time.

Although no definitive conclusions can be drawn regarding the clinical role of cortical lesions, the presence of focal cortical pathology in patients at early stages of MS is indicated by our findings.

Acknowledgments

The authors thank the following persons who provided helpful guidance and support in image acquisition: MR imaging technicians J. Black and R. Hill from the NIH-MRI Research Facility, NINDS-NIH, Bethesda, Md, and E. Condon from the NIMH-NIH. Postprocessing analysis was highly facilitated by J.M. Solomon and T.A. Tasciyan from Medical Numerics, Inc, Sterling, Va; J.M. McAuliffe from Biomedical Imaging Research Services Section at the NIH; J.L. Ostuni from the NINDS-NIH; and R.C. Reynolds from Scientific and Statistical Computing Core from Scientific and Statistical Computing Core NIMH-Intramural Research Programs, Department of Health and Human Services, NIH. Dr. N.D. Richert is gratefully acknowledged for CELs identification. Neuroimaging Branch-NINDS clinicians (Drs. Bibiana Bielekova, Gregg Blevins, Carlos Mora, and Unsong Oh) as well as nurses Helen

Griffith and Jennifer McCartin are acknowledged for performing the clinical work-ups of patients. Mr. Roger Stone is acknowledged for image storing/collections and for data base maintenance.

We are finally but mostly indebted to all our patients and their families as well as all the healthy volunteer subjects for their time, cooperation, and availability.

References

1. Brownell B, Hughes JT. **The distribution of plaques in the cerebrum in multiple sclerosis.** *J Neurol Neurosurg Psychiatry* 1962;25:315–20
2. Kidd D, Barkhof F, McConnell R, et al. **Cortical lesions in multiple sclerosis.** *Brain* 1999;122:17–26
3. Peterson JW, Bo L, Mork S, et al. **Transected neuritis, apoptotic neurons, and reduced inflammation in cortical multiple sclerosis lesions.** *Ann Neurol* 2001; 50:389–400
4. Bo L, Vedeler CA, Nyland HI, et al. **Subpial demyelination in the cerebral cortex of multiple sclerosis patients.** *J Neuropathol Exp Neurol* 2003;62:723–32
5. Brink BP, Veerhuis R, Breij EC, et al. **The pathology of multiple sclerosis is location-dependent: no significant complement activation is detected in purely cortical lesions.** *J Neuropathol Exp Neurol* 2005;64:147–55
6. Geurts JJ, Bo L, Pouwels PJ, et al. **Cortical lesions in multiple sclerosis: combined postmortem MR imaging and histopathology.** *AJNR Am J Neuroradiol* 2005;26:572–77
7. Boggild MD, Williams R, Haq N, et al. **Cortical plaques visualised by fluid-attenuated inversion recovery imaging in relapsing multiple sclerosis.** *Neuroradiology* 1996;38(suppl 1):10–13
8. Filippi M, Yousry T, Baratti C, et al. **Quantitative assessment of MRI lesion load in multiple sclerosis: a comparison of conventional spin-echo with fast fluid-attenuated inversion recovery.** *Brain* 1996;119:1349–55
9. Gawne-Cain ML, O'Riordan JI, Thompson AJ, et al. **Multiple sclerosis lesion detection in the brain: a comparison of fast fluid-attenuated inversion recovery and conventional T2-weighted dual spin echo.** *Neurology* 1997;49:364–70
10. Rovaris M, Filippi M, Minicucci L, et al. **Cortical/subcortical disease burden and cognitive impairment in patients with multiple sclerosis.** *AJNR Am J Neuroradiol* 2000;21:402–08
11. Bakshi R, Ariyaratana S, Benedict RH, et al. **Fluid-attenuated inversion recovery magnetic resonance imaging detects cortical and juxtacortical multiple sclerosis lesions.** *Arch Neurol* 2001;58:742–48
12. Geurts JJ, Pouwels PJ, Uitdehaag BM, et al. **Intracortical lesions in multiple sclerosis: improved detection with 3D double inversion-recovery MR imaging.** *Radiology* 2005;236:254–60
13. Kurtzke JF. **Rating neurologic impairment in multiple sclerosis: an expanded disability status scale (EDSS).** *Neurology* 1983;33:1444–52
14. Sled JG, Zijdenbos AP, Evans AC. **A non-parametric method for automatic correction of intensity non-uniformity in MRI data.** *IEEE Trans Med Imaging* 1998;17:87–97
15. Pezawas L, Verchinski BA, Mattay VS, et al. **The brain-derived neurotrophic factor val66met polymorphism and variation in human cortical morphology.** *J Neurosci* 2004;24:10099–102
16. Yuen KK. **A note on Winsorized t.** *Appl Stat* 1971;20:297–304
17. Cox RW. **AFNI: software for analysis and visualization of functional magnetic resonance neuroimages.** *Comput Biomed Res* 1996;29:162–73
18. Cox RW, Jesmanowicz A. **Real-time 3D image registration for functional MRI.** *Magn Reson Med* 1999;42:1014–18
19. Talairach J, Tournoux P. *Co-planar Stereotaxic Atlas of the Human Brain: 3-Dimensional Proportional System: An Approach to Cerebral Imaging.* New York: Thieme; 1988
20. Jenkinson M, Smith S. **A global optimization method for robust affine registration of brain images.** *Med Image Anal* 2001;5:143–56
21. Bagnato F, Jeffries N, Richert ND, et al. **Evolution of T1 black holes in patients with multiple sclerosis imaged monthly for 4 years.** *Brain* 2003;126:1782–89
22. Bagnato F, Butman JA, Mora C, et al. **Conventional magnetic resonance imaging features in patients with tropical spastic paraparesis.** *J Neurovirol* 2005;11: 525–34
23. Pham DL, Xu C, Prince JL. **A survey of current methods in medical image segmentation.** In: Yarmush ML, Diller KR, Toner M, eds. *Annual Review of Biomedical Engineering, Vol. 2.* Palo Alto, Calif: Annual Reviews; 2000:315–37.
24. Smith SM, De Stefano N, Jenkinson M, et al. **Normalized accurate measurement of longitudinal brain change.** *J Comput Assist Tomogr* 2001;25:466–75
25. Pelletier D, Garrison K, Henry R. **Measurement of whole-brain atrophy in multiple sclerosis.** *J Neuroimaging* 2004;14(suppl 3):11–19
26. Rudick RA, Fisher E, Lee JC, et al. **Use of the brain parenchymal fraction to measure whole brain atrophy in relapsing-remitting MS: Multiple Sclerosis Collaborative Research Group.** *Neurology* 1999;53:1698–704
27. Kutzelnigg A, Lucchinetti CF, Stedelmann C, et al. **Cortical demyelination and diffuse white matter injury in multiple sclerosis.** *Brai*n. 2005;128:2705–12
28. Chard DT, Griffin CM, McLean MA, et al. **Brain metabolite changes in cortical grey and normal-appearing white matter in clinically early relapsing–remitting multiple sclerosis.** *Brain* 2002;125:2342–52
29. Kapeller P, MC Lean MA, Griffin CM, et al. **Preliminary evidence for neuronal damage in cortical grey matter and normal-appearing white matter in short duration relapsing–remitting multiple sclerosis: a quantitative MR spectroscopic imaging study.** *J Neurol* 2001;248:131–38
30. Sailer M, Fischl B, Salat D, et al. **Focal thinning of the cerebral cortex in multiple sclerosis.** *Brain* 2003;126:1734–44
31. Chen JT, Narayanan S, Collins DL, et al. **Relating neocortical pathology to disability progression in multiple sclerosis using MRI.** *NeuroImage* 2004;23: 1168–75
32. Fischl B, Dale AM. **Measuring the thickness of the human cerebral cortex from magnetic resonance images.** *Proc Natl Acad Sci U S A* 2000;97:11050–55